WILEY VCH

RESEARCH ARTICLE

Synthesis and Conformational Analysis of α,β-Dichlorocarbonyl Compounds

Shunta Kobayashi,[a] Nurcahyo Iman Prakoso,[a,b] Xin Zheng,[c] Shin-ichiro Noro,[a,c] Masaru Hashimoto,[d] Tatsuya Morozumi,[e] and Taiki Umezawa * [a,c]

[a] Mr. S. Kobayashi, Dr. N. I. Prakoso, Prof. S. Noro, Prof. T. Umezawa
Division of Environmental Materials Science, Graduate School of Environmental Science, Hokkaido University, N10W5 Sapporo 060-0810, Japan,
e-mail: umezawa@ees.hokudai.ac.jp,

[b] Dr. N. I. Prakoso
Chemistry Department, Universitas Islam Indonesia, Indonesia.

[c] Dr. X. Zheng, Prof. S. Noro, Prof. T. Umezawa
Section of Environmental Material Science, Faculty of Environmental Earth Science, Hokkaido University, N10W5 Sapporo 060-0810, Japan,

[d] Prof. M. Hashimoto
Faculty of Agriculture and Life Science, Hirosaki University, Hirosaki 036-8561, Japan,

[e] Dr. T. Morozumi
Section of chemistry, Faculty of Science, Hokkaido University, N10W8 Sapporo 060-0810, Japan,

Supporting information for this article is given via a link at the end of the document.

Abstract: α,β-Dichlorocarbonyl compounds were synthesized by facile dichlorination of α,β-unsaturated amides with TCIA-PPh_3 and the resultant amides were converted to ketones. Conformational analyses of the products were performed to confirm our previous hypothesis regarding vicinal dichlorinated carbonyl compounds. The compounds exhibited ^{1}H NMR signals with large coupling constants (7-11 Hz) for the 1,2-*anti*-configuration and small coupling constants (3-4 Hz) for the 1,2-*syn*-configuration. The *syn*-pentane interaction enabled rational conformational analysis of the α,β-dichlorinated carbonyl compounds, although some interesting exceptions were observed. Consideration of these conformations is helpful in assigning relative configurations of α,β-dihalogenated carbonyl compounds in general.

Introduction

1,2-Dichloroalkanes are often found in pharmaceutical candidates [1] and natural products [2] with unique biological activities. After the characterization of chlorosulfolipids (CSLs), [3] which are natural products containing a highly chlorinated long alkyl chain, various diastereoselective or stereospecific preparations of 1,2-dichloroalkanes were developed.[4] In addition to the dichlorination reaction for CSLs, dichlorination, bromination for other natural products and pharmaceuticals have been demonstrated, affording α,β-dihalocarbonyl compounds. [5] Assigning the relative configuration of the resultant compounds is crucial for understanding their biological properties. These assignments have been mainly conducted by (1) derivatization to a known product, [5d,5f,5h,5j,5l,5m] (2) X-ray diffraction, [5e,5k] or (3) *J*-based configuration analysis, called the JBCA method, developed by Murata. [6] However, some synthetic papers have not assigned the relative configurations of the 1,2-dichlorinated compounds. [5a,5c]

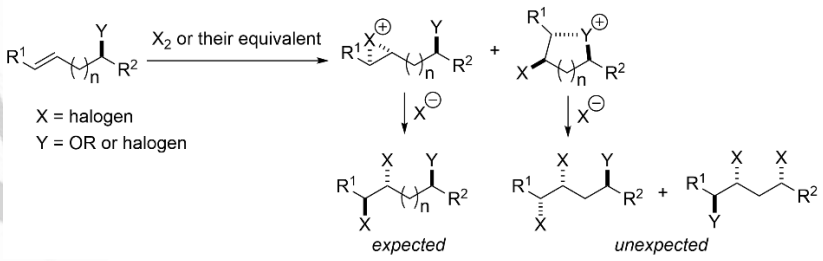

Figure 1. Unexpected pathway in dihalogenation reaction.

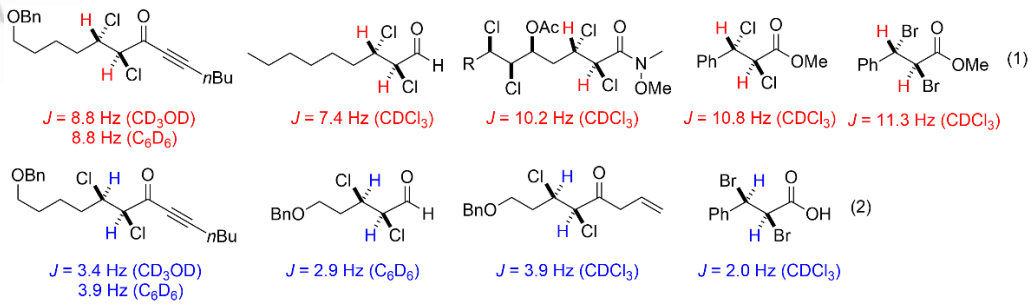

Figure 2. Characteristic coupling constants of α,β-dichlorocarbonyl compounds.

In most studies, these assignment methods have been employed only for a representative compound, and relative configurations of the other products were then implied to avoid complicated and multiple procedures for full assignments. It is desired that the relative configurations for all products are confirmed in the developed conditions since neighboring effects by alkoxy or halide groups often occur to form oxonium[7] or halonium[8] ion intermediates (Figure 1). These intermediates induce rearrangement products or a mixture of diastereomers even in a stereospecific reaction such as the dihalogenation reaction of a double bond.

We found the characteristic coupling constants (*J* values) for α,β-dichlorocarbonyl compounds during the synthesis of mytilipin C, [9] a member of the CSL family. [10] These coupling constants can easily be calculated from routine ^{1}H NMR spectra. Specifically, a large coupling constant (7-11 Hz) is observed for the 1,2-*anti*-configuration (Figure 2, eq 1), while a small coupling constant (3-4 Hz) is seen in the 1,2-*syn*-configuration (Figure 2, eq 2). NMR spectra of α,β-dichlorocarbonyl compounds synthesized by other research groups exhibit the same trend even in the case of α,β-dibromocarbonyl compounds. [11] To validate our hypothesis, we synthesized compounds depicted in Figure 3 using newly developed methods. These compounds are expected to be intermediates toward CSLs. The coupling constants for the products and conformational analyses are discussed.

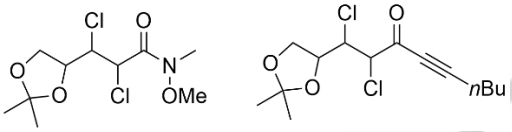

Figure 3. Synthetic targets in this study.

Results and Discussion

Synthesis of α,β-Dichlorinated Weinreb Amide 3

The synthesis of Weinreb amide **3** commenced with commercially available racemic **1**, which was homologated through TEMPO oxidation and subsequent Wittig reaction in a one-pot operation to give *E*-unsaturated amide **2a** and *Z*-unsaturated amide **2b** as a separable mixture, isolated using silica gel column chromatography (Scheme 1). Convenient dichlorination of the unsaturated amides was next investigated according to the pioneering work by Yoshimitsu. [12] The results for **2a** are summarized in Table 1. The original condition with *N*-chlorosuccinimide (NCS, **A**) as a Cl^+ source resulted in the formation of **3a** and **3b** as an inseparable diastereomeric mixture with low yield, despite attempts with longer reaction times and higher temperatures (entries 1 and 2). We next investigated the alternative Cl^+ sources, *N*-chlorosaccharin (NCSC, **B**) and trichloroisocyanuric acid (TCIA, **C**), proceeding through the same reaction pathway as NCS. NCSC, having a stronger electron-withdrawing group than NCS, improved the efficiency of the dichlorination reaction to 48% combined yield at room temperature (entry 3). TCIA afforded a much higher yield compared to NCS or NCSC (entry 4). Increasing the equivalents of TCIA slightly enhanced the yield (entry 5). The diastereoselectivity observed in these reactions was around 70:30 (**3a**:**3b**). This reaction could be successfully scaled up without loss of chemical yield (entry 7).

Scheme 1. Synthesis of unsaturated amides **2**.

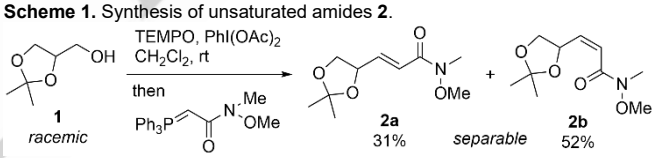

Table 1. Optimization of dichlorination reaction with *E*-olefin **2a** [a]

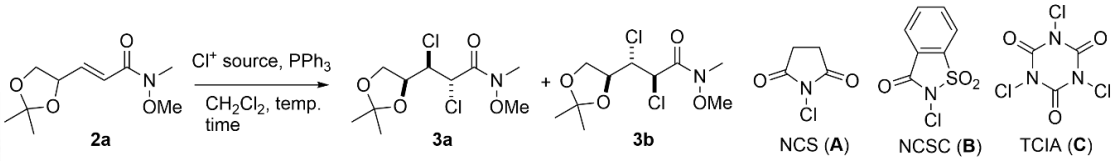

Entry	Cl^+ source (equiv.)	PPh_3 (equiv.)	Temp. (°C)	Time (h)	Combined yield[b] (%)	Ratio[c] (**3a**:**3b**)
1	**A** (3.0)	1.5	rt	7	4	70:30
2	**A** (5.0)	2.5	40	18	39	75:25
3	**B** (3.0)	1.5	rt	7	48	69:31
4	**C** (1.0)	1.5	0 to rt	7	62	70:30
5	**C** (1.5)	1.5	0 to rt	5	67	72:28
6	**C** (1.0)	1.5	0	24	62	69:31
7[d]	**C** (1.0)	1.5	0 to rt	7	70	67:33

[a] Reactions were carried out on a 0.20 mmol scale for optimization. [b] Isolated yield after silica gel chromatography. [c] Ratio was estimated by ^{1}H NMR after silica gel chromatography. [d] 306 mg (1.42 mmol) of **2a** was used.

Similar reactivity to **2a** was observed when **2b** was employed for the dichlorination reaction, as shown in Table 2. The reactions with NCS and NCSC resulted in lower yields than that with TCIA (entries 1-4). The reaction on a gram-scale of **2b** afforded a high yield of 80% (entry 5). The mixture of **3c** and **3d** could not be separated by silica gel column chromatography. The selectivity corresponded to the previous reports with *Z*-olefins. [4a]

Although all diastereomers were prepared efficiently, it was challenging to separate the mixture using silica gel chromatography. After exhaustive attempts, the isolation of all diastereomers was achieved through careful recrystallization. For the mixture of **3a** and **3b**, a solvent system with CH_2Cl_2-hexane selectively crystallized **3a**. After several crystallization steps, almost all of **3a** could be recovered as crystals, resulting in pure **3b**. The diastereomers **3c** and **3d** were also resolved by recrystallization with CH_2Cl_2-hexane as solvents. Crystallization of **3d** first occurred, and after removal of almost all of **3d** through several crystallization operations, **3c** was subjected to another recrystallization to afford pure **3c**. The relative configurations of **3a**, **3c** and **3d** were unambiguously assigned by single crystal X-ray diffraction analyses, as shown in Figure 4. Interestingly, the crystals of **3a** and **3c** were racemic, while the crystal of **3d** had a chiral space group of $P2_12_12_1$ and included only one enantiomer by spontaneous resolution. Additionally, the conformations of all diastereomers of **3** were examined by JBCA analysis, which suggested the same conformation as observed in X-ray analysis.

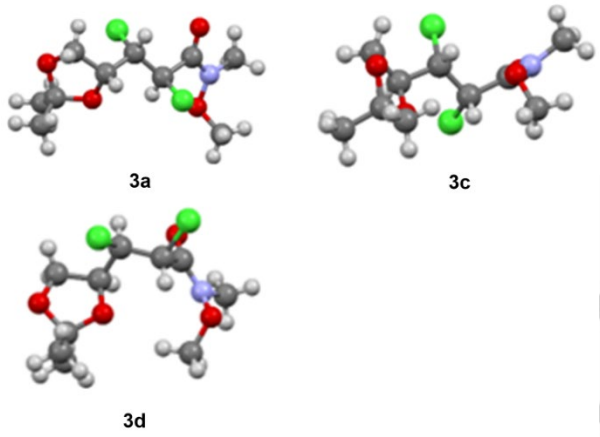

Figure 4. X-ray analysis of **3a**, **3c** and **3d**. The dark gray, light gray, red, blue and green colors represent carbon, hydrogen, oxygen, nitrogen and chlorine, respectively.

Coupling Constants and Conformational Analyses

With all diastereomers of **3** in hand, ^{1}H NMR spectra were measured to confirm our hypothesis, expecting a large ^3J (H_2, H_3) coupling constant for the 2,3-*anti*-configuration and a small coupling constant for the 2,3-*syn*-configuration. The results with $CDCl_3$ are shown in Table 3. While **3a**, **3b** and **3c** followed the hypothesis, **3d** exhibited a different trend.

Table 3. Coupling constants for **3** in $CDCl_3$.

	3a (2,3-*anti*)	**3b** (2,3-*anti*)	**3c** (2,3-*syn*)	**3d** (2,3-*syn*)
^3J (H_2,H_3)	10.7 Hz	8.4 Hz	3.0 Hz	9.8 Hz
^3J (H_3,H_4)	2.0 Hz	4.6 Hz	9.2 Hz	2.3 Hz

Table 2. Optimization of dichlorination reaction with *Z*-olefin **2b** [a].

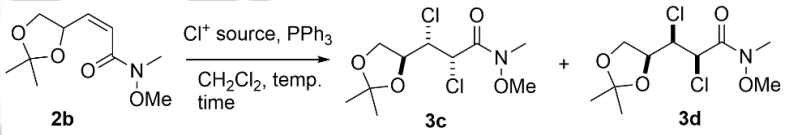

Entry	Cl^+ source (equiv.)	PPh_3 (equiv.)	Temp. (°C)	Time (h)	Combined yield[b] (%)	Ratio[c] (**3c**:**3d**)
1	**A** (3.0)	1.5	rt	7	0.7	22:78
2	**A** (5.0)	2.5	40	24	30	26:74
3	**B** (3.0)	1.5	rt	7	37	31:69
4	**C** (1.0)	1.5	0 to rt	7	75	31:69
5[d]	**C** (1.0)	1.5	0 to rt	7	80	17:83

[a] Reactions were carried out on a 0.20 mmol scale for optimization. [b] Isolated yield after silica gel chromatography. [c] Ratio was estimated by ^{1}H NMR after silica gel chromatography. [d] 3.00 g (13.9 mmol) of **2b** was used.

We evaluated the difference in these coupling constants based on the *syn*-pentane interaction, proposed by Hoffmann. [13] The concept of the *syn*-pentane interaction is described in Figure 5. Among some representative conformers **A**-**C** of *n*-pentane illustrated in eq 3, conformers **A** (C_2-C_3: *anti*; C_3-C_4: *anti*) and **B** (C_2-C_3: *anti*; C_3-C_4: *syn*) are thought to be favored. Conformer **C** (C_2-C_3: *syn*; C_3-C_4: *syn*) is disfavored due to steric repulsion between terminal methyl groups, similar to the 1,3-diaxial repulsion found in cyclohexane. Next, the conformations of 2,4-substituted (alkyl, Cl or OR) pentane are considered (eq 4). Conformer **D** (C_2-C_3: *syn*; C_3-C_4: *anti*) is believed to be favored over conformers **E** (C_2-C_3: *anti*; C_3-C_4: *anti*) and **F** (C_2-C_3: *syn*; C_3-C_4: *anti*) that generate steric repulsion between substituents or methyl groups and a substituent. Thus, zig-zag conformers such as **A** and **E** are not always favored due to the unfavorable *syn*-pentane interaction.

Figure 5. *Syn*-pentane interaction.

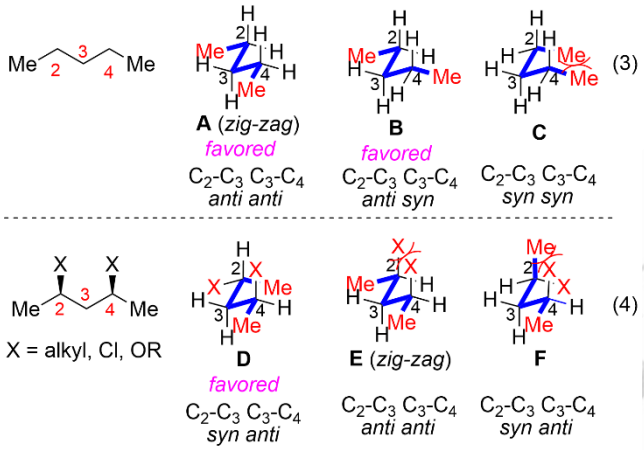

With the concept of the *syn*-pentane interaction in mind, the favored conformations of **3a-d** are discussed as shown in Figure 6. The zig-zag conformations (C_2-C_3: *anti*; C_3-C_4: *anti*) of **3a-d** serve as standards. The zig-zag conformation of **3a** is thought to be favored due to the absence of steric repulsion between larger substituents such as alkyl, chloride or alkoxy groups. In this conformation, vicinal protons H_2 and H_3 are in an *anti*-relationship, with a large coupling constant (10.7 Hz). The H_3/H_4-*gauche* conformer is also favorable, with a small coupling constant (2.0 Hz). This conformation corresponds to those from the X-ray and JBCA analyses (see Supporting Information). The conformation of **3b** is analyzed based on the *syn*-pentane interaction. In the zig-zag conformer, steric repulsion between the chloride at C_2 and the alkoxy group at C_4 is possible, causing the C_3-C_4 bond to rotate to minimize the repulsion. In this conformer, large and small coupling constants are expected for H_2/H_3 and H_3/H_4, respectively, which are identical to those observed. The case of *syn*-diastereomers, **3c** and **3d**, is also considered. In **3c**, the zig-zag conformation is favored since the *syn*-pentane interaction is not expected to occur. X-ray analysis also supports the zig-zag conformation. The conformation of **3d** is similar to that of **3b**, yielding the *syn*-pentane interaction in the zig-zag conformation. However, rotation of the C_2-C_3 bond occurred to avoid the *syn*-pentane interaction. We believe this rotation induced the unexpected coupling constant (9.8 Hz). DFT calculations (CAM-B3LYP[4]/6-31G*) to estimate the rotation of the C_2-C_3 and C_3-C_4 bonds could not reproduce the experimental results in **3c** as shown in boxes. Although these results do not completely match our hypothesis, the presence of the alkoxy group at C_4 (or γ-position of carbonyl group) is anticipated to complicate the conformation through the *syn*-pentane interaction. Additionally, the amide group often induces conformers which may be why the conformation of

Figure 6. Conformational analysis of **3** and calculated conformations in boxes.

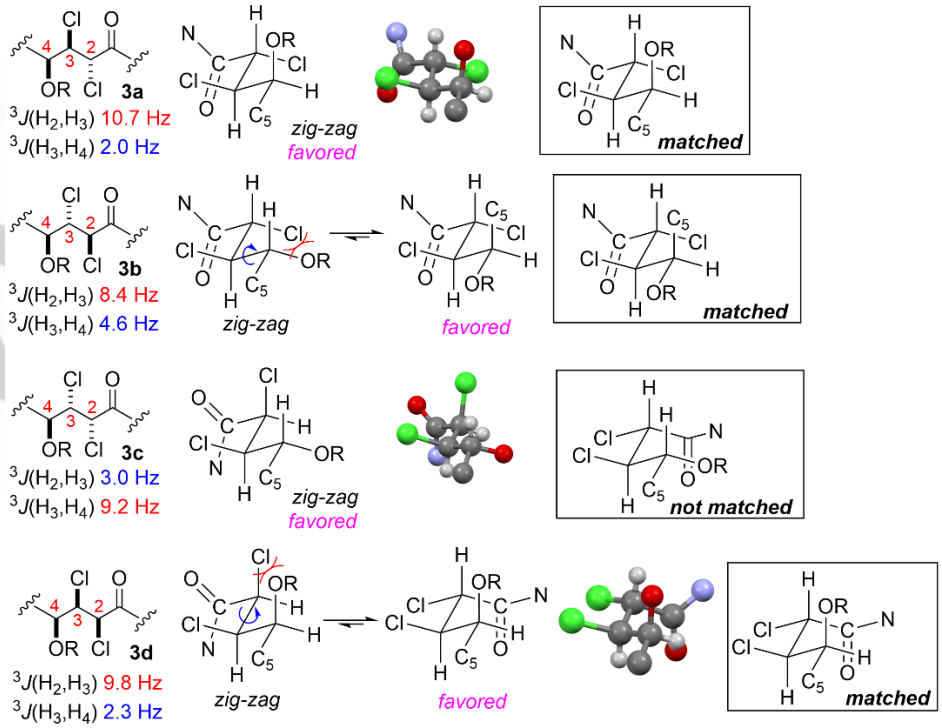

calculated amide **3c** was different from that of the experimental result. DFT-based chemical shifts moderately supported the above arguments, although these calculations could not specify the configuration of **3c**. This would be an example that shows the limitations of the GIAO methodology.[14]

Synthesis and Analysis of α,β-Dichlorinated Ketones

To investigate another α,β-dichlorinated carbonyl compound, all diastereomers of Weinreb amides **3** were converted to the corresponding ketones **4** using our previous method as shown in Table 4. [15] Addition of commercially available $LaCl_3$·2LiCl was crucial, as a considerable amount of side product **12** resulting from an elimination reaction was observed in the absence of $LaCl_3$·2LiCl. The coupling constants for synthetic **4** are summarized in Table 5. The values for **4a** and **4c** corresponded to those for amide **3**, likely due to the favorable zig-zag conformations. On the other hand, the small and large values for **4b** were reversed from those for **3b**, and intermediate values were observed for $^3J(H_2,H_3)$ and $^3J(H_3,H_4)$ of **4d**. Conformational considerations for **4b** and **4d** are described in Figure 7. As indicated in Figure 6, in the **b** and **d** series, the zig-zag conformation was not preferred, since rotation of the C_2-C_3 or C_3-C_4 bond occurred to avoid the *syn*-pentane interaction. In the conformation of **4b**, rotation of the C_2-C_3 bond occurred, resulting in the observed coupling constants. In the case of **4d**, we believe an equilibrium between the C_2-C_3 and C_3-C_4 bond rotations leads to the intermediate values. Both conformers are favored by considering the *syn*-pentane interaction.

DFT calculations (CAM-B3LYP[4]/6-31G*) were performed for ketones **4a-d**. The most abundant conformer suggested for each isomer is shown in boxes. Interestingly, the calculated conformations reproduced the experimental ones based on the coupling constants, although only one of the two possible conformers was proposed for **4d**. These results suggest the potential for stable conformations in acyclic systems.

Table 4. Synthesis of ketone **4**.

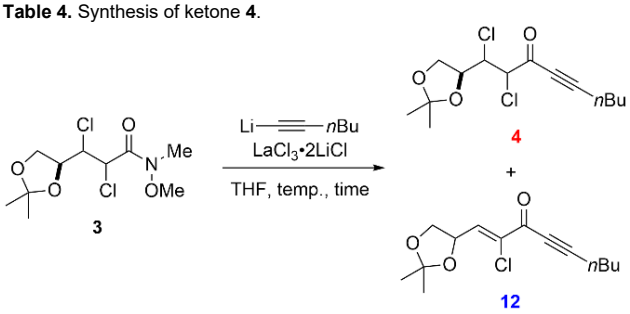

Entry	Substrate	Temp. (°C)	Time (min)	Ratio (**3**:**4**:**12**)[a] and combined yield (**4**+**12**)
1	**3a**	0	10	0:93:7, 62%
2	**3b**	0	10	51:47:2, 36%
3	**3c**	–40	30	32:67:1, 67%
4	**3d**	–40	30	0:95:5, 77%

[a] Isolated yield after silica gel chromatography.

Table 5. Coupling constants of **4** in $CDCl_3$.

	4a (2,3-*anti*)	**4b** (2,3-*anti*)	**4c** (2,3-*syn*)	**4d** (2,3-*syn*)
$^3J(H_2,H_3)$	10.6 Hz	3.3 Hz	2.0 Hz	5.2 Hz
$^3J(H_3,H_4)$	1.9 Hz	8.5 Hz	9.6 Hz	5.4 Hz

Figure 7. Conformational analysis and calculated conformations in boxes.

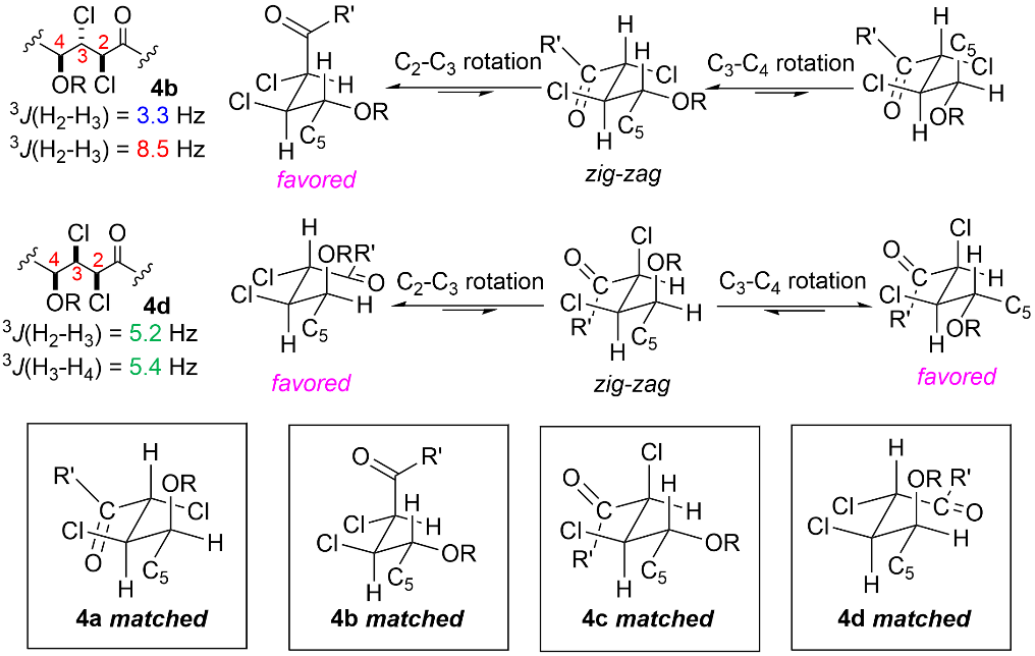

Conclusion

In summary, we described the facile dichlorination reaction of α,β-unsaturated amides with the TCIA and PPh_3 system, along with the successful conversion of the resultant amides to ketones in the presence of $LaCl_3$·2LiCl. Conformational analyses were shown to validate our hypothesis: large coupling constants (7-11 Hz) in the 1,2-*anti*-configuration and small coupling constants (3-4 Hz) in the 1,2-*syn*-configuration for α,β-dichlorinated carbonyl compounds. The *syn*-pentane interaction enabled rational conformational analyses for α,β-dichlorinated carbonyl compounds, although our hypothesis may not always apply to more complex compounds. Nevertheless, the current considerations and DFT calculations regarding these conformational analyses are expected to aid in determining the relative configurations not only for α,β-dichlorinated carbonyl compounds but also for α,β-dihalogenated carbonyl compounds.

Experimental Section

General: The IR spectra were recorded on a JASCO FTIR-4100 Type A spectrometer (JASCO corporation, Tokyo, Japan) using a NaCl cell. ESI-MS were obtained on a JEOL JMS-700TZ (JEOL Ltd., Tokyo, Japan) or BRUKER DALTONICS micro TOF-HS focus spectrometer (Bruker Japan Ltd., Yokohama, Japan). The ^{1}H NMR and ^{13}C NMR spectra were recorded using a JNM-ECZR 500 (500 MHz and 126 MHz) spectrometer (JEOL Ltd., Tokyo, Japan). Chemical shifts were reported in ppm relative to $CHCl_3$ in $CDCl_3$ for ^{1}H NMR (δ = 7.26) and ^{13}C NMR (δ = 77.0). Splitting patterns for ^{1}H NMR were designated as "s, d, t, q, m, dt, dd, and td". These symbols indicate "singlet, doublet, triplet, quartet, multiplet, doublettriplet, doubletdoublet, and tripletdoublet" respectively. All commercially obtained reagents were employed as received. Analytical TLC was carried out using pre-coated silica gel plates (Wako TLC Silicagel 70F_{254}, FUJIFILM Wako Pure Chemical Corporation, Osaka, Japan). Wakogel 60N 63-212 μm was used for column chromatography.

General procedure for the preparation of dichloride 3: To a solution of **2** (1.0 equiv.) in DCM (0.20 M) were added TCIA (1.0 equiv.) and PPh_3 (1.5 equiv.) at 0 °C to rt for 7 h. The reaction mixture was quenched with Na_2SO_3 aq and $NaHCO_3$ aq, extracted with DCM washed with brine dried over Na_2SO_4 filtered, and concentrated under reduced pressure. The residue was purified by silica gel column chromatography (Hexane:EtOAc = 95:5 then 90:10) to give mixture of **3**.

General procedure for the preparation of ketone 4: To a solution of 1-hexyne (3.1 equiv.) in THF (1.1 mL) were added *n*BuLi (3.0 equiv.) at –20 °C to give acetylide. After 30 minutes, a solution of $LaCl_3$-2LiCl (1.5 equiv.) was added. After 10 minutes, a solution of **3** (1.0 equiv.) in THF was added. The mixture was stirred for 10 minutes at suggested temperature, quenched with 4.00 M HCl in 1,4-dioxane (5.0 equiv.) then excess of H_2O, extracted with EtOAc, washed with brine, dried over Na_2SO_4, filtered and concentrated *in vacuo*. The residue was purified by silica gel column chromatography (Hexane:EtOAc:AcOH = 98:1:1) to give a mixture of **4a** and **12**.

X-ray diffraction analysis: Single crystal X-ray diffraction measurements were performed using a RIGAKU XtaLAB P200 diffractometer with Mo Kα radiation (λ = 0.71075 Å) at 173 K. The crystal structures were solved using SHELXT[16] and refined by full-matrix least-squares techniques on F^2 using SHELXL-2018 (ver. 2018/3).[17] Anisotropic refinement was applied to all atoms except for hydrogen atoms.
Deposition Numbers 2343550 (**3a**), 2343549 (**3c**) and 2343548 (**3d**) contain the supplementary crystallographic data for this paper. These data are provided free of charge by the joint Cambridge Crystallographic Data Centre and Fachinformationszentrum Karlsruhe Access Structures service.

General procedures of DFT calculation; The (2*S**,3 *S**,4 *S**)-isomer **3c** was built using the Spartan'20 program, and the diastereomers at C-2 and C-4 were generated using the built-in function.[18] Each isomer underwent a conformation search with MMFF,[19] retaining the conformers within 40 kJ/mol of the global minimum conformer. Conformer narrowing was conducted by (i) structural optimizations based on 6-31G*, setting the threshold at 40 kJ/mol from the global minimum conformer, and (ii) energy calculation without altering the geometries based on CAM-B3LYP[20]/6-31G*, with the threshold set at 15 kJ/mol from the global minimum conformer. The remaining candidate conformers were optimized using CAM-B3LYP/6-31G* and subsequently subjected to NMR chemical shifts calculation using the same DFT-models. The program automatically converted the calculated tensors to chemical shifts, followed by empirical corrections. The energy of each conformer was estimated using CAM-B3LYP[21]/6-311+G(2df,2p)//CAM-B3LYP/6-31G*. The NMR chemical shifts of each conformer were averaged, taking into account the Boltzmann distribution based on the SCF energy.
The calculated ^{13}C and ^{1}H NMR chemical shifts of each diastereomer were then analyzed with root mean square deviation (RMSD, in ppm) from the experimental data and DP4 probability, applying Goodman's parameters (σ: 2.306 ppm for ^{13}C, 0.185 ppm for ^{1}H, v: 11.38 for ^{13}C, 14.18 for ^{1}H). The details of conformer narrowing and the chemical shifts of each conformer are documented in the SI file named 'computational calculation.xlsx' in SI.

Supporting Information

Experimental procedures, characterization data, X-ray data, calculation results and spectral data of all compounds are given in the Supporting Information.

Acknowledgements

This work was funded by a Grant-in-Aid for Young Scientists (B) [23710245] and a Grant-in-Aid for Scientific Research (C) [16K01908] from the Japan Society for the Promotion of Science (JSPS). The authors thank FORTE Science Communications (https://www.forte-science.co.jp/) for English language editing.

Keywords: Chlorine substituents • NMR spectroscopy • coupling constants • carbonyl compounds • conformational analysis

1. (a) S. Omura, H. Tomoda, K. Kimura, D. Z. Zhen, H. Kumagai, K. Igarashi, N. Imamura, Y. Takahashi, Y. Tanaka, Y. Iwai, *J. Antibiot.* **1988**, *41*, 1769-1773; (b) H. Miyadera, K. Shiomi, H. Ui, Y. Yamaguchi, R. Masuma, H. Tomoda, H. Miyoshi, A. Osanai, K. Kita, S. Ōmura, *Proc. Natl. Acad. Sci*. **2003**, *100*, 473-477; (c) T. Schafhauser, L. Jahn, N. Kirchner, A. Kulik, L. Flor, A. Lang, T. Caradec, D. P. Fewer, K. Sivonen, W. J. H. van Berkel, P. Jacques, T. Weber, H. Gross, K. -H. van Pée, W. Wohlleben, J. Ludwig-Müller, *Proc. Natl. Acad. Sci*. **2019**, *116*, 26909-26917.
2. (a) G. W. Gribble, *Mar. Drugs*. **2015**, *13*, 4044-4136; (b) E. M. Antunes, A. F. Afolayan, M. T. Chiwakata, J. Fakee, M. G. Knott, C. E. Whibley, D. T. Hendricks, J. J. Bolton, D. R. Beukes, *Phytochemistry*. **2011**, *72*, 769–772.
3. (a) J. L. Chen, P. J. Proteau, M. A. Roberts, W. H. Gerwick, D. L. Slate, R. H. Lee, *J. Nat. Prod*. **1994**, *57*, 524–527; (b) P. Ciminiello, E. Fattorusso, M. Forino, S. Magno, M. D. Rosa, A. Ianaro, R. Poletti, *J. Org. Chem.* **2001**, *66*, 578–582; (c) T. Kawahara, Y. Kumaki, T. Kamada, T. Ishii, T. Okino, *J. Org. Chem*. **2009**, *74,* 6016–6024; (d) A. R. Pereira, T. Byrum, G. M. Shibuya, C. D. Vanderwal, W. H. Gerwick, *J. Nat. Prod*. **2010**, *73*, 279–283.
4. (a) G. M. Shibuya, J. S. Kanady, C. D. Vanderwal, *J. Am. Chem. Soc.* **2008**, *130*, 12514–12518; (b) T. Yoshimitsu, N. Fukumoto, T. Tanaka, *J. Org. Chem.* **2009**, *74*, 696–702; (c) Y. Kamada, Y. Kitamura, T. Tanaka, T. Yoshimitsu, *Org. Biomol. Chem.* **2013**, *11*, 1598–1601; (d) M. L. Landry, D. X. Hu, G. M. McKenna, N. Z. Burns, *J. Am. Chem. Soc.* **2016**, *138*, 5150–5158; (e) C. Nilewski, R. W. Geisser, M.-O. Ebert, E. M. Carreira, *J. Am. Chem. Soc.* **2009**, *131*, 15866−15876; (f) P. Sondermann, E. M. Carreira, *J. Am. Chem. Soc.* **2019**, *141*, 10510−10519.
5. (a) N. B. Barhate, A. S. Gajare, R. D. Wakharkar, A. V. Bedekar, *Tetrahedron* **1999**, *55*, 11127–11142; (b) A. Y. B. Ángel, E. F. Bragança, E. E. Alberto, *ChemistrySelect* **2019**, *4*, 11548–11552; (c) L. Xingchao, W. Lu, Z. Jianping, *Chin. J. Chem.* **2011**, *29*, 2097–2100; (d) T. Kitamura, Y. Tazawa, M. H. Morshed, S. Kobayashi, *Synthesis* **2012**, *44*, 1159–1162; (e) H. Xue, H. Tan, D. Wei, Y. Wei, S. Lin, F. Liang, B. Zhao, *RSC Adv.* **2013**, *3*, 5382–5385; (f) P. Swamy, M. M. Reddy, M. A. Kumar, M. Naresh, N. Narender, *Synthesis* **2014**, *46*, 251–257; (g) R. Ding, S. Huang, Q. Wang, Y. Liu, B. Sun, H. Tian, *Synthetic Communications* **2020**, *50*, 2319–2330; (h) P. Lian, W. Long, J. Li, Y. Zheng, X. Wan, *Angew. Chem. Int. Ed*. **2020**, *59*, 23603–23608; (i) X. Dong, J. L. Roeckl, S. R. Waldvogel, B. Morandi, *Science* **2021**, *371*, 507–514; (j) T. B. Poynder, S. D. Houston, J. L. Dutton, *Eur. J. Org. Chem*. **2021**, *19*, 2788–2791; (k) F. Liu, N. Wu, X. Cheng, *Org. Lett.* **2021**, *23*, 3015–3020; (l) L. Wang, L. Zhai, J. Chen, Y. Gong, P. Wang, H. Li, X. She, *J. Org. Chem.* **2022**, *87*, 3177–3183; (m) Z. Dağalan, R. Koçak, A. Daştan, B. Nişancı, *Org. Lett*. **2022**, *24*, 8261–8264.
6. N. Matsumori, D. Kaneno, M. Murata, H. Nakamura, K. Tachibana, *J. Org. Chem.* **1999**, *64*, 866–876.
7. T. Yoshimitsu, N. Fukumoto, R. Nakatani, N. Kojima, T. Tanaka, *J. Org. Chem.* **2010**, *75*, 5425–5437.
8. (a) M. L. Landry, X. X. Hu, G. M. McKenna, N. Z. Burns, *J. Am. Chem. Soc.* **2016**, *138*, 5150–5158; (b) P. Sondermann, E. M. Carreira, *J. Am. Chem. Soc.* **2019**, *141*, 10510–10519.
9. T. Umezawa, N. I. Prakoso, K. Tsuji, Y. Ogura, T. Sato, F. Matsuda, *Bull. Chem. Soc. Jpn.* **2022,** *95*, 1491–1500.
10. (a) T. Umezawa, M. Shibata, K. Kaneko, T. Okino, F. Matsuda, *Org. Lett.* **2011**, *13*, 904-907; (b) T. Umezawa, M. Shibata, R. Tamagawa, F. Matsuda, *Org. Lett.* **2019**, *21*, 7731-7735; (c) W. -J. Chung, J. S. Carlson, C. D. Vanderwal, *J. Org. Chem.* **2014**, *79*, 2226–2241; (d) W. -J. Chung, J. S. Carlson, K. D. Bedke, C. D. Vanderwal, *Angew. Chem., Int. Ed.* **2013**, *52*, 10052–10055.
11. (a) X. Zeng, C. Gong, J. Zhang, J. Xie, *RSC Adv.* **2016**, *6*, 85182–85185; (b) Y. Tan, S. Luo, D. Li, N. Zhang, S. Jia, Y. Liu, W. Qin, C. E. Song, H. Yan, *J. Am. Chem. Soc.* **2017**, *139*, 6431–6436.
12. T. Yoshimitsu, N. Fukumoto, R. Nakatani, N. Kojima, T. Tanaka, *J. Org. Chem.* **2010**, *75*, 5425-5437.
13. R. Göttlich, B. C. Kahrs, J. Krüger, R. W. Hoffmann, *Chem. Commun***. 1997**, *3*, 247-252.
14. G. Barone, D. Duca, A. Silvestri, L. Gomez-Paloma, R. Riccio, G. Bifulco, *Chem. Eur. J.* **2002**, *8*, 3240-3245.
15. N. I. Prakoso, F. Matsuda, T. Umezawa, *Org. Biomol. Chem***. 2021**, *19*, 7822-7826.
16. G. M. Sheldrick, SHELXT–Integrated space-group and crystal-structure determination. *Acta Cryst.* **2015**, *A71*, 3–8.
17. G. M. Sheldrick, Crystal structure refinement with SHELXL. *Acta Cryst.* **2015**, *C71*, 3–8.
18. Wavefunction-Inc., *Tutorial and User's Guide, Spartan '20 for Windows, Macintosh and Linux*. Wavefunction inc., : 2019.
19. T. A. Halgren, *J. Comp. Chem.* **1996,** *17*, 490-519.
20. J.-D. Chai, M. Head-Gordon, *Phys. Chem. Chem. Phys.* **2008,** *10*, 6615-6620.
21. N. Mardirossian, M. Head-Gordon, *Phys. Chem. Chem. Phys.* **2014,** *16*, 9904-9924.

Entry for the Table of Contents

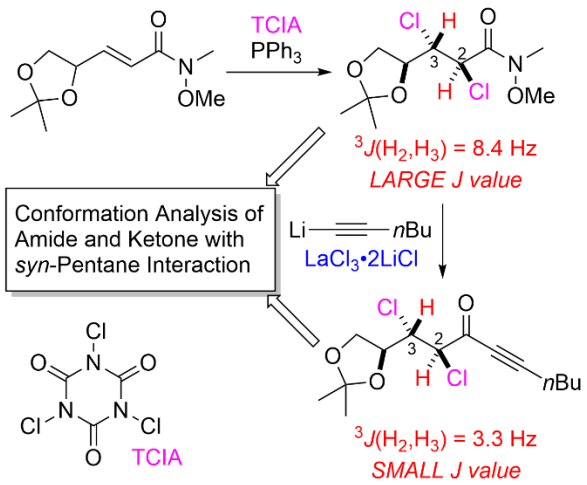

Facile dichlorination reactions of α,β-unsaturated amides with TCIA-PPh_3 and conversion of the resultant amides to ketones are described to confirm our previous hypothesis with ^{1}H NMR: large coupling constants for 1,2-*anti*-dichlorides and small coupling constants for 1,2-*syn*-dichlorides. Unique conformational analyses of the products are discussed with the *syn*-pentane interaction although the hypothesis was not always found.